Received: 21 January 2020 | Revised: 18 September 2020 | Accepted: 27 October 2020

DOI: 10.1002/stc.2665

RESEARCH ARTICLE

WILEY

Assessment of the tuned mass damper inerter for seismic response control of base-isolated structures

Chiara Masnata[1] | **Alberto Di Matteo**[1] | **Christoph Adam**[2] | **Antonina Pirrotta**[1]

[1]Dipartimento di Ingegneria, Università degli Studi di Palermo, Palermo, Italy

[2]Unit of Applied Mechanics, University of Innsbruck, Innsbruck, Austria

Correspondence
Christoph Adam, Unit of Applied Mechanics, University of Innsbruck, Technikerstr. 13, 6020 Innsbruck, Austria.
Email: christoph.adam@uibk.ac.at

Summary

In this paper, the hybrid control of structures subjected to seismic excitation by means of tuned mass damper inerter (TMDI) and base-isolation subsystems is studied with the aim of improving the dynamic performance of base-isolated structures by reducing the displacement demand of the isolation subsystem. The seismic performance of TMDI hybrid controlled structures is investigated in a comparative study, considering simple isolated systems and systems equipped with other absorber devices such as the tuned mass damper (TMD) and the tuned liquid column damper (TLCD). The TMDI has been optimized by performing a simplified approach based on minimizing the base-isolation subsystem displacement variance, which provides simple analytical formulae for a quick definition of the TMDI parameters. The reliability of this approach is demonstrated by a comparison with a more accurate and computationally complex numerical optimization procedure. The control performance of three types of hybrid controlled structures exposed to a set of 44 recorded ground motions is investigated. Numerical results show that the TMDI can more efficiently control the structural response of low-damped isolated structures, even compared to the TMD and the TLCD.

KEYWORDS

base-isolation system, hybrid control, optimal design, seismic excitation, tuned mass damper inerter

1 | INTRODUCTION

In order to reduce the vulnerability of civil structures against seismic-induced vibrations, an effective and widely employed passive control strategy is related to the installation of isolators between the structure and its foundation.[1] The introduction of a flexible support by means of isolators, like elastomeric and/or sliding bearings, yields structures with a longer dominant natural period with respect to the correspondent structure fixed at the base. Therefore, considering the typical earthquake frequency content, such a measure leads to lower seismic forces and reduced deformations and accelerations in the entire superstructure. However, the several advantages of equipping the structure with a base-isolation system come at expenses of a substantial concentration of displacements in the isolation layer with detrimental effects on the base-isolation subsystem.[2]

This drawback has recently been addressed by the use of the so-called hybrid control strategies, which combine the base-isolation system with other passive control devices, usually attached to the base plate of the isolated structure and designed to minimize the base displacements without compromising the dynamic performance of the main structure with respect to other structural quantities (interstory drift and floor deformations/accelerations). In this regard, the idea of connecting a freely oscillating secondary mass to the base slab by means of a spring and a dashpot dates back the studies of Yang et al,[3] who proposed the use of the tuned mass damper (TMD) at the base. Subsequently, researches on the potentiality of base-isolation systems combined with TMD in its traditional or nontraditional form have exponentially increased.[4-6] Although there are few real-world examples of applied hybrid control strategies,[7] it has been widely proved, even experimentally, that these strategies are effective means for improving the seismic performance of isolated buildings.[8] Moreover, many optimization procedures have been proposed to determine the optimal TMD parameters for different types of external excitation inputs.[3,9,10]

In this framework, a number of researchers have also explored the coupling of base-isolated systems with liquid-based devices such as the tuned liquid damper (TLD)[11] and the tuned liquid column damper (TLCD).[12] These are passive vibration control systems that substantially dissipate structural vibrations through the motion of a liquid contained in the device itself. In a TLCD with constant cross-section, the natural frequency of oscillation, according to theoretical models, depends only on the total length of the liquid inside a U-shaped container.[13] This feature makes TLCDs particularly well suited to systems characterized by a predominant first mode with a very low fundamental natural frequency, as in the case of base-isolated structures. Because, unlike traditional TMDs, the equations governing the TLCD controlled systems response is nonlinear and the definition of the optimal TLCD parameters is time-consuming in a predesign phase,[12,14] many studies have introduced some formulations to choose the optimal parameters of TLCD in a direct way and some experimental tests have been conducted to prove the reliability of these procedures.[15] Furthermore, the effectiveness of TLCDs in reducing the base displacement demand has been experimentally assessed in Furtmüller et al[16] by small-scale tests on isolated structural models.

Note that the base displacements of base-isolated systems can be further reduced by the combined use of the classical TMD with inerter-based devices.[17] Currently, three different types of inerter are essentially under investigation: the rack and pinion inerter, the ball screw inerter, and the fluid inerter.[18-20] However, in all these cases, the operating principle of the inerter is the same. The inerter is simply a lightweight device provided with two terminals. The inertial force developed at the extremities of the inerter is proportional to the relative acceleration between its end points and to a constant of proportionality. This is denoted as inertance, which has the same dimension of a mass. It can be seen as a kind of virtual mass that can reach great values, even up to 200 times more than the real mass of the device. In this way, the inerter is able to generate a sort of mass amplification effect. Hence, by connecting an inerter to a classical TMD, the TMD mass and thus its effectiveness can be easily amplified without any weight penalty. In particular, when the inerter is placed between the TMD mass and the ground (considering the case of the TMD located at the base of an isolated structure), it constitutes an improved version of the TMD generally referred to as tuned mass damper inerter (TMDI), which has only recently been introduced in the field of civil engineering.[21-25] Many studies have already highlighted the reduction of base displacements and roof displacements of isolated buildings achieved by placing the TMDI at the base, and many different criteria based on both kinematic and energy-related indices have been established to optimally design the TMDI.[20,25]

Recently, a simplified analytical solution for the optimal design of the TMDI for base-isolated structures has been proposed in Matteo et al,[26] considering an approach based on minimizing the base displacement variance of the base-isolation subsystem and some simplifying hypotheses such as Gaussian white noise as base excitation, assuming a linear undamped single degree of freedom (SDOF) system to model the base-isolated structure.

On this basis, the present study aims to assess the effectiveness of the TMDI in improving the seismic performance of base-isolated buildings by extending the optimization procedure presented in Matteo et al.[26] Specifically, as a first novel contribution of this study, the accuracy of the simplified analytical solution introduced in Matteo et al[26] is investigated by a comparison with a more complex and accurate numerical procedure applied directly to the more general case of a damped multi-degree-of-freedom (MDOF) isolated structure. Moreover, it is worth stressing that in Matteo et al,[26] the seismic performance of a five-story isolated structure equipped with a TMDI has been analyzed only for two seismic actions. In the present paper, the comparison of the structural responses of the system with and without TMDI is performed considering a set of 44 recorded ground motions as base excitation, with different magnitudes on several soil site classes (both soft and stiff soils are considered). Additionally, the effectiveness of the TMDI placed at the base is compared with other devices such as the TLCD and TMD. Furthermore, in order to verify the reliability of the simplified optimization procedure, presented in Matteo et al[26] for only one structural type, this study extends its application

to other types of base-isolated structures with different characteristics. Finally, the influence of the damping ratio of the base-isolated structure on the control performance is thoroughly investigated both in time and frequency domain.

2 | PROBLEM FORMULATION

Consider a planar structure with n dynamic degrees-of-freedom, separated through a base-isolation subsystem from the foundation, as shown in Figure 1a for the example of a shear-frame structure. The response of such a base-isolated structure, subjected to a seismic horizontal ground acceleration $\ddot{x}_g(t)$, is governed by the following set of equations:

$$\begin{aligned} &M_{tot}\ddot{x}_b(t) + \mathbf{r}^T\mathbf{M}\ddot{\mathbf{x}}(t) + C_b\dot{x}_b + K_b x_b = -M_{tot}\ddot{x}_g(t), \\ &\mathbf{M}(\mathbf{r}\ddot{x}_b(t) + \ddot{\mathbf{x}}(t)) + \mathbf{C}\dot{\mathbf{x}}(t) + \mathbf{K}\mathbf{x}(t) = -\mathbf{M}\mathbf{r}\ddot{x}_g(t), \end{aligned} \tag{1}$$

where $\mathbf{M}$, $\mathbf{C}$, and $\mathbf{K}$ are respectively the $n \times n$ mass, damping, and stiffness matrix of the main structure, $\mathbf{x}$ is the vector containing the nodal deformations of the structure with respect to the base plate, $\mathbf{r} = [1...1]^T$ is the $(n\times 1)$ quasi-static influence vector, M_b, C_b, and K_b are respectively mass, damping, and stiffness of the base-isolation subsystem (modeled as a linear system) and $M_{tot} = M_b + \mathbf{r}^T\mathbf{M}\mathbf{r}$ is the total mass of the system. The base displacement relative to the ground is denoted as $x_b(t)$, and a dot over a variable denotes a derivation with respect to time t.

Next, consider the base-isolated system equipped with a TMDI device, as depicted in Figure 1b, which aims at reducing the displacement demand of the isolation subsystem. The TMDI mass is attached to the base plate with one end of the inerter device connected to the ground and the other to TMDI mass, which is free to move. The displacement of the TMDI relative to the base is denoted as $x_d(t)$. Let m_d, b, c_d, and k_d be respectively the mass, the inertance, the damping, and the stiffness of the TMDI. The equations of motion of this $n + 2$ degrees-of-freedom system are derived as

$$\begin{aligned} &(M_{tot} + m_d + b)\ddot{x}_b(t) + (m_d + b)\ddot{x}_d(t) + \mathbf{r}^T\mathbf{M}\ddot{\mathbf{x}}(t) + C_b\dot{x}_b(t) + K_b x_b(t) = -(M_{tot} + m_d)\ddot{x}_g(t), \\ &(m_d + b)\ddot{x}_b(t) + (m_d + b)\ddot{x}_d(t) + c_d\dot{x}_d(t) + k_d x_d(t) = -m_d\ddot{x}_g(t), \\ &\mathbf{M}(\mathbf{r}\ddot{x}_b(t) + \ddot{\mathbf{x}}(t)) + \mathbf{C}\dot{\mathbf{x}}(t) + \mathbf{K}\mathbf{x}(t) = -\mathbf{M}\mathbf{r}\ddot{x}_g(t). \end{aligned} \tag{2}$$

It is worth stressing that when $b = 0$ in Equation (2), the equations of motion of a base-isolated MDOF system equipped with a classical TMD are recovered.

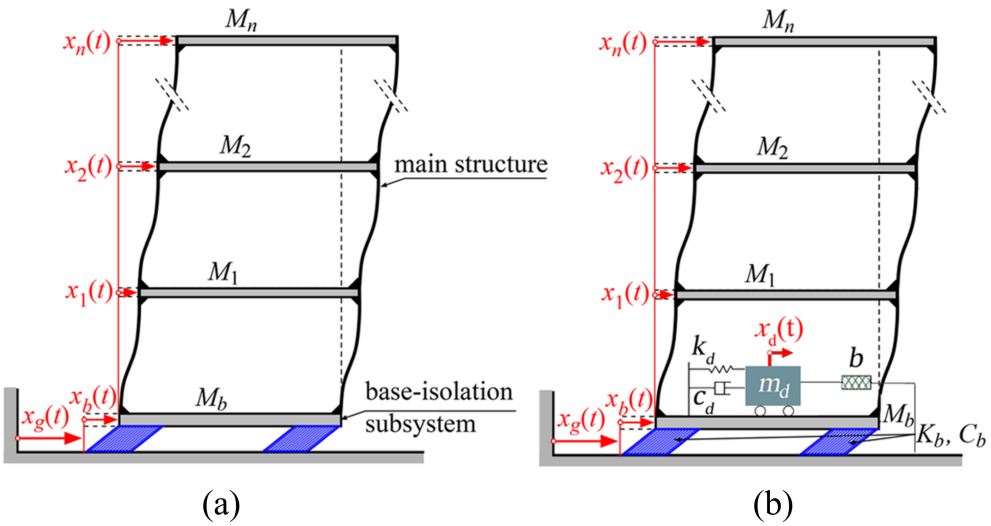

FIGURE 1 (a) Base-isolated MDOF shear frame; (b) hybrid controlled MDOF shear frame with TMDI

3 | OPTIMAL TMDI PARAMETERS

The optimization procedure taken into account for tuning the herein considered devices refers to the approach developed for the TLCD and TMDI cases in previous studies.[26-28] For the sake of the application of this optimization procedure, Equation (2) are rewritten as

$$\begin{gathered}(1+\mu_d+\beta)\ddot{x}_b(t)+(\mu_d+\beta)\dot{x}_d(t)+\frac{1}{M_{tot}}\mathbf{r}^T\mathbf{M}\ddot{\mathbf{x}}(t)+2\omega_b\zeta_b\dot{x}_b(t)+{\omega_b}^2x_b(t)=-(1+\mu_d)\ddot{x}_g(t),\\ \ddot{x}_b(t)+\ddot{x}_d(t)+2\omega_d\zeta_d\dot{x}_d(t)+{\omega_d}^2x_d(t)=-\frac{\mu_d}{\mu_d+\beta}\ddot{x}_g(t),\\ \mathbf{M}(\mathbf{r}\ddot{x}_b(t)+\ddot{\mathbf{x}}(t))+\mathbf{C}\dot{\mathbf{x}}(t)+\mathbf{K}\mathbf{x}(t)=-\mathbf{M}\mathbf{r}\ddot{x}_g(t),\end{gathered} \tag{3}$$

where $\zeta_b=C_b/(2M_{tot}\omega_b)$ and $\omega_b=\sqrt{K_b/M_{tot}}$ are the damping ratio and the frequency of the base-isolation subsystem respectively, while ω_d , ζ_d, μ_d, and β are the circular natural frequency, the damping ratio, the mass ratio, and the inertance ratio characterizing the stand-alone TMDI,

$$\omega_d=\sqrt{\frac{k_d}{m_d+b}},\ \zeta_d=\frac{c_d}{2\omega_d(m_d+b)},\ \mu_d=\frac{m_d}{M_{tot}},\ \beta=\frac{b}{M_{tot}}. \tag{4}$$

Although the TMDI is characterized by four parameters (ω_d, ζ_d, μ_d, and β), the optimum design usually deals with the determination of two parameters, specifically, the frequency or, as customary, the tuning ratio $\nu_d=\omega_d/\omega_b$ and the damping coefficient ζ_d, since the mass ratio and the inertance ratio of the TMDI are generally fixed by design constraints. The herein adopted procedure derives the optimal parameters of the control device by minimizing the base displacement variance of the base-isolation subsystem on the base of some simplifying hypotheses.

It is worth underlining that linear models and linear analysis can be used when the structure is provided with linear isolation, although it should be noted that isolators with high damping commonly become strongly nonlinear. However, when there is a high degree of modal isolation, simplified system models may be adopted to approximate the structural behavior of base-isolated structures. In this case, the first mode and damping of the isolated structure governs the seismic response of the entire system. As a consequence, the main structure may be represented by a rigid mass when assessing the seismic responses of its first vibration mode.[4-6,11,12] Since the displacements of the superstructure are orders of magnitude lower than those on the isolation level, the first hypothesis reasonably concerns to assume the entire base-isolated structure as a single degree-of-freedom (SDOF) system that has the total mass of the original structure, stiffness and damping of the base-isolation system, and only the degree-of-freedom with respect to the displacement of the base plate. In this manner, the original system of equations of motion of an MDOF isolated structure equipped with the control device is significantly reduced to only two equations. Second, the excitation force is considered as a zero-mean Gaussian white noise process characterized by constant one-sided power spectrum with amplitude G_0. In the literature, this assumption is commonly adopted to obtain a close approximation of the probabilistic nature of an earthquake for the design phase of passive control systems.[23,29] Indeed, this hypothesis leads to a mathematical simplification which allows achieving approximated solutions of the optimal TMDI parameters. Therefore, at this stage, by assuming the input as described by a stationary stochastic process and the entire base-isolated building as an SDOF system, the original system in Equation (3) can be recast as

$$\begin{gathered}(1+\mu_d+\beta)\ddot{X}_b(t)+(\mu_d+\beta)\ddot{X}_d(t)+2\omega_b\zeta_b\ddot{X}_b(t)+{\omega_b}^2X_b(t)=-(1+\mu_d)\ddot{X}_g(t),\\ \ddot{X}_b(t)+\ddot{X}_d(t)+2\omega_d\zeta_d\ddot{X}_d(t)+{\omega_d}^2X_d(t)=-\frac{\mu_d}{\mu_d+\beta}\ddot{X}_g(t),\end{gathered} \tag{5}$$

where capital letters are used because $\ddot{X}_g(t)$ is a white noise process, and hence, displacements and their derivatives are stochastic processes too. In light of the last consideration, the response also takes the form of a zero mean stationary process, whose complete description is given by its covariance matrix which is satisfied using the Lyapunov equation.[28] A more detailed study of the mathematical steps leading from Equation (5) to the response in the Lyapunov form can

be found in Matteo et al.[26] According to the procedure detailed in Matteo et al,[26] the base displacement steady-state variance can be expressed in a closed form as

$$\sigma_{X_b}^2 = \frac{\pi G_0}{4\zeta_{X_b}\omega_b^3}, \zeta_{X_b} = \frac{N_Z}{D_Z}. \tag{6}$$

Because only the term ζ_{X_b} depends on the TMDI parameters, the optimal values of ν_d and ζ_d, which minimize $\sigma_{X_b}^2$, can be equivalently found directly looking for the minimum of the function

$$\phi(\nu_d, \zeta_d) = \frac{1}{\zeta_{X_b}}. \tag{7}$$

The numerator N_Z and denominator D_Z of ζ_{X_b} are given by

$$\begin{aligned} N_Z &= \zeta_d{}^2(\beta+\mu_d)\nu_d + 4\zeta_b{}^2\zeta_d\nu_d{}^2 + \zeta_b\zeta_d\left[1-2\nu^2 + 4\zeta_d{}^2(1+\beta+\mu_d)\nu_d{}^2 + (1+\beta+\mu_d)^2\nu_d{}^4\right] + \\ &\quad + \zeta_b{}^2\left[(\beta+\mu_d)\nu_d{}^3 + 4\zeta_d{}^2(1+\beta+\mu_d)\nu_d{}^3\right] \end{aligned} \tag{8}$$

$$\begin{aligned} D_Z &= \zeta_d(1+\mu_d)\left[4\zeta_d{}^2(1+\mu_d)(1+\beta+\mu_d)\nu_d{}^2 + \beta(-1+\mu_d) + (1+\mu_d)(-2+4\zeta_b{}^2+\mu_d)\right]\nu_d{}^2 + \\ &\quad + \zeta_d + \zeta_d(1+\mu_d)^2(1+\beta+\mu_d)^2\nu_d{}^4 + \zeta_b\nu_d\left[\mu_d{}^2 + (1+\mu_d)^2(\beta+\mu_d)\nu_d{}^2\right] + \\ &\quad + 4\zeta_b\zeta_d{}^2(1+\mu_d)^2\nu_d[1+(1+\beta+\mu_d)\nu_d{}^2]. \end{aligned} \tag{9}$$

The minimum of the function $\phi(\nu_d, \zeta_d)$ in Equation (7) can be found directly by well-known numerical algorithms already contained in many commercial software (for example, through FindMinimum in Mathematica or fminsearch in MATLAB environment). However, in order to determine formulae of design parameters that are easier to handle, a further approximation can be introduced. As a matter of fact, in many optimization procedures, it is common to assume the base-isolation subsystem as undamped (i.e., for $\zeta_b \to 0$).[24] This is a classical approach used for the optimization of passive control systems in structural engineering, which led in the past to optimal design parameters of a number of passive control systems such as TMD, TLCD, and TLD. Thus, aiming to achieve an analytical solution easy to implement, the design parameters can be determined, by assuming ζ_b be equal to zero, in a closed-form as[26]

$$\nu_{d,opt} = \left[\frac{2(1+\mu_d)(1+\beta+\mu_d)^2}{2+\beta+\mu_d(1-\beta-\mu_d)}\right]^{-\frac{1}{2}}, \tag{10}$$

$$\zeta_{d,opt} = \frac{1}{2}\left[2 + \frac{1}{\beta+\mu_d} + \frac{5+4\beta+5\mu_d}{\beta(\mu_d-3)+(\mu_d-4)(1+\mu_d)}\right]^{-\frac{1}{2}}. \tag{11}$$

In this way, the optimal values of the TMDI design parameters can be evaluated in a straightforward manner, and their values do not directly depend on the input power spectral density (PSD), nor on the base-isolation subsystem parameters. Notably, although the main structure and the base-isolation subsystem have been assumed to be linear, the herein developed analysis would be equally applicable by utilizing, for instance, an equivalent linearization technique to partially take into account for the effect of the nonlinearity.[12]

Note that the above described procedure has been derived considering an equivalent SDOF system and a white noise base excitation, thus leading to the simplified analytical expressions in Equations (10) and (11) for the optimal parameters. Clearly, the optimization procedure could have been also carried out directly on the complete MDOF system, using the aforementioned Lyapunov equation or other techniques.[29] In this case, however, considering the complexity of the problem at hand, a numerical optimization procedure would have been required. Observe that this numerical solution would depend on the specific parameters of the MDOF system. Further, as addressed in Di Matteo et al,[26] a more realistic model of earthquake ground accelerations could also be taken into account by means of models such as the Kanai–Tajimi filtered spectrum and/or Clough–Penzien spectrum to simulate the seismic excitation. The introduction of these filters implies a more complicated problem formulation in terms of Lyapunov equation, thus requiring again a numerical

optimization procedure. However, as demonstrated in Di Matteo et al,[26] the optimal values in Equations (10) and (11) closely agree with those obtained by using the aforementioned filters for different soil conditions. Thus, the above approach can effectively be considered as a reliable tool even for different model of earthquake excitation.

4 | ACCURACY OF THE OPTIMAL PARAMETERS

In order to investigate on the accuracy of the above introduced optimization procedure, the hypothesis assuming the entire base-isolated structure as an undamped SDOF system is now removed, and a comparison is made with the optimal values obtained numerically considering the original MDOF isolated structure. Note that maintaining the assumption of the white noise process, the steady-state variance of the base displacement of the base-isolation subsystem can be expressed as follows:

$$\sigma_{X_b}^2 = \int_0^\infty |H_{X_b}(\omega)|^2 G_0 d\omega, \tag{12}$$

where $H_{X_b}(\omega)$ denote the base-isolation subsystem displacement transfer function of the structure equipped with the TMDI. This function can be expressed in a closed form as described in Appendix A1. However, considering the complexity of the transfer function expression (see Appendix A1 for details), calculated on the complete damped system in Equation (3), the research of the optimal parameters of the TMDI, ν_d and ζ_d, which minimize the variance in Equation (12), requires a rather cumbersome numerical iterative procedure. Note that the involved integral in Equation (12) depends both on the structural properties and the parameters of the device, which are still unknown. Therefore, because in this case, both many degrees of freedom and the damping of the base isolation system have been considered, unlike the proposed simplified solution in Equations (10) and (11), an iterative procedure is necessary.

Specifically, first, the standard deviation of the base displacement of the base-isolation subsystem is evaluated by fixing arbitrary values of ν_d and ζ_d within proper bounds.[23] Then, the minimum value of $\sigma_{X_b}^2$ and the corresponding parameters ν_d and ζ_d are searched. In this way, the procedure is repeated and the values of ν_d and ζ_d are iteratively updates until no significant differences emerge between consecutive iterations. In this respect, considering a reference set of parameters, which in turn are varied in a wide range of values, the particle-swarm optimization (PSO) method[30] is used to find the couple of values (ν_d, ζ_d) that minimizes the base-isolation displacement variance $\sigma_{X_b}^2$ of the complete MDOF system in Equation (2).

Specifically, the benchmark MDOF structure considered for the numerical simulations is base-isolated five-story planar frame ($n = 5$) analyzed in De Domenico and Ricciardi,[23] which is not a shear-type frame. As far as the structural properties are concerned, each one of the first four floors has a lumped mass equal to $M_j = 60 \times 10^3$ kg (for $j = 1, ..., 4$), and the mass of the fifth story is $M_5 = 50 \times 10^3$ kg. The natural frequencies of the superstructure are ω_j[rad/s] $= [12.5, 33.2, 56.1, 79.5, 112.2]$ and the system is assumed to be a classically damped structure with damping ratio of each mode is $\zeta_j = 0.02$. The basement mass, the damping ratio and natural frequency of the base-isolation subsystem are $M_b = 50 \times 10^3$ kg, $\zeta_b = 0.1$ and $\omega_b = \pi$ rad/s, respectively. Further, in order to properly design the TMDI to be connected to the base-isolated structure, a constant value of the PSD equal to $G_0 = 0.002$ has been set. For this value of PSD and for this kind of structure, according to the closed-form solutions in Equations (10) and (11), the optimal design parameters $\nu_{d,opt} = 0.781$ and $\zeta_{d,opt} = 0.264$ have been calculated by setting the mass ratio $\mu_d = 0.05$ and an inertance ratio $\beta = 0.3$ of the TMDI device.

In Table 1, the optimal design parameters $\nu_{d,\,opt}$ and $\zeta_{d,\,opt}$, obtained from the approximated solutions in Equations (10) and (11), are listed against those determined through the aforementioned iterative solution, for various values of the system parameters, together with the corresponding percentage differences and the normalized base-isolation displacement variance expressed as

$$\varepsilon_{X_b} = \sigma_{X_b}^2 / \sigma_{X_0}^2, \tag{13}$$

where $\sigma_{X_0}^2$ is the base-isolation displacement variance of the system without any devices, and the error ε_{X_b} estimates the discrepancy between the closed-form formulae and the results obtained from the PSO algorithm applied on the complete base-isolated five-story frame.

TABLE 1 Comparison of optimal TMDI design parameters $\nu_{d,\,opt}$ and $\zeta_{d,\,opt}$ (Reference set of values: $\beta = 0.3$, $\mu_d = 0.05$, $\zeta_b = 0.1$, $\omega_b = \pi$, $\zeta_1 = 0.02$, $G_0 = 0.002$)

		$\nu_{d,\,opt}$ Proposed approach	$\nu_{d,\,opt}$ Iterative solution	Err. (%)	$\zeta_{d,\,opt}$ Proposed approach	$\zeta_{d,\,opt}$ Iterative solution	Err. (%)	ε_{X_b} Proposed approach	ε_{X_b} Iterative solution	Err. (%)
	0.1	0.878	0.825	−6.438	0.184	0.179	−3.975	0.518	0.510	−1.417
β	0.2	0.826	0.784	−5.363	0.230	0.223	−4.384	0.444	0.440	−0.906
	0.3	0.781	0.747	−4.551	0.264	0.257	−1.930	0.397	0.395	−0.659
	0.4	0.741	0.709	−4.496	0.292	0.282	−3.396	0.363	0.362	−0.523
	0.03	0.798	0.769	−3.797	0.258	0.248	−3.981	0.393	0.391	−0.505
μ_d	0.05	0.781	0.743	−5.092	0.264	0.258	−2.435	0.397	0.395	−0.667
	0.07	0.764	0.722	−5.836	0.271	0.262	−3.164	0.401	0.398	−0.832
	0.10	0.739	0.692	−6.919	0.279	0.275	−1.705	0.407	0.403	−1.079
	0.05	0.781	0.760	−2.709	0.264	0.258	−2.368	0.244	0.243	−0.374
ζ_b	0.1	0.781	0.740	−5.460	0.264	0.256	−3.277	0.397	0.395	−0.668
	0.15	0.781	0.727	−7.333	0.264	0.258	−2.688	0.504	0.499	−0.897
	0.2	0.781	0.710	−9.919	0.264	0.250	−5.594	0.582	0.576	−1.069
	0.01	0.781	0.744	−4.975	0.264	0.259	−1.845	0.392	0.389	−0.665
ζ_1	0.02	0.781	0.744	−4.863	0.264	0.256	−3.277	0.397	0.395	−0.668
	0.1	0.781	0.744	−4.885	0.264	0.257	−2.991	0.436	0.433	−0.668
	0.2	0.781	0.745	−4.828	0.264	0.257	−2.811	0.481	0.478	−0.667
	$1 \cdot 10^{-4}$	0.781	0.744	−4.966	0.264	0.256	−3.106	0.397	0.395	−0.668
G_0	$5 \cdot 10^{-4}$	0.781	0.744	−4.966	0.264	0.256	−3.106	0.397	0.395	−0.668
	$1 \cdot 10^{-3}$	0.781	0.744	−4.966	0.264	0.256	−3.106	0.397	0.395	−0.668
	$5 \cdot 10^{-3}$	0.781	0.744	−4.966	0.264	0.256	−3.106	0.397	0.395	−0.668

It should be noticed that, because the closed-form solutions in Equations (10) and (11) are not functions of G_0, ζ_1, ζ_b, then $\nu_{d,\,opt}$ and $\zeta_{d,\,opt}$, deduced by the proposed approach, are not affected by any value fluctuations due to their changes. Similarly, because the systems are linear, variations of G_0 do not influence the coordinates, $\nu_{d,\,opt}$ and $\zeta_{d,\,opt}$, corresponding to the minimum of the variance calculated with the iterative procedure by means of Equation (12).

Moreover, Table 1 shows that there are small discrepancies between the two approaches with regard to the optimal tuning ratio $\nu_{d,\,opt}$, whereas for the optimal damping ratio $\zeta_{d,\,opt}$, there are large differences. However, as highlighted in the last columns of Table 1, the two procedures lead to similar values for the parameter ε_{X_b}. Note that, as expected, the minus sign for these errors indicates that higher control is achieved when the optimal parameters are evaluated by the iterative procedure. Nevertheless, since very small discrepancies are obtained in terms of ε_{X_b}, and given the significant reduction in computational effort achieved with the proposed straightforward procedure, the above approach can effectively be considered a powerful and reliable tool that can be used to evaluate the optimal design parameters.

Next, in order to investigate on the influence of the nonstationary nature of real ground motions on the reliability of the approximated solution, the control performances of the base-isolated structure equipped with a TMDI are examined using different selected recorded accelerograms extracted by the collection of the 44 recorded far-field ground motions of the FEMA P-695-FF set.[31] In fact, in the previous analysis, a stationary white noise process was used as a model for base acceleration to derive the optimal design parameters with the minimal computational cost. Obviously, real earthquake ground motions are neither stationary nor they have a constant PSD as in the case of the white noise. Therefore, for each of the FEMA P-695-FF 44 records, the displacement relative to the ground, total acceleration, and interstory drift ratio of the base-isolation subsystem and of the main structure are determined for both the base-isolated structure and the base-isolated structure controlled by the TMDI. In this regard, Figure 2 shows comparison of the profiles of the median (line with circle markers) of the peak response quantities of the base-isolated structure with the TMDI numerically optimized (red dashed line) and with the TMDI optimized via the approximated solution (blue solid line). For the

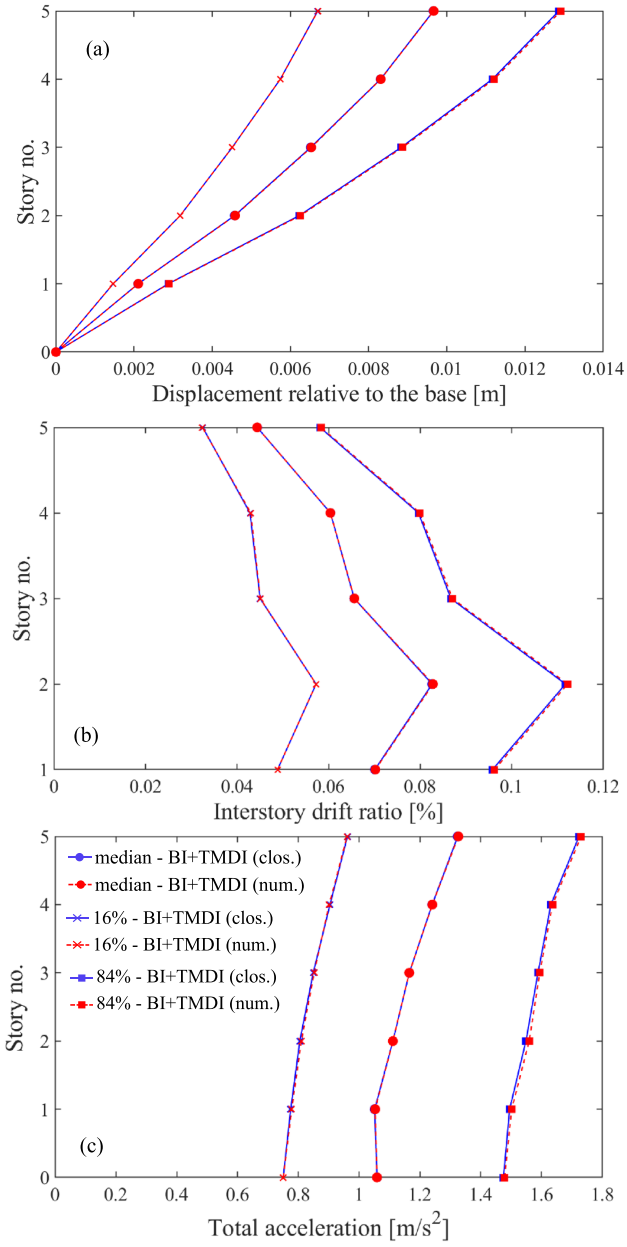

FIGURE 2 Response profiles for flexible five-story hybrid controlled structure with TMDI optimized via the approximated solution (blue solid line) and with TMDI optimized by the numerical approach (red dashed line) subjected to the 44 FEMA P-695-FF records: circles—median; crosses—16th percentile; squares—84th percentiles; (a) peak floor displacement relative to the base; (b) peak floor interstory drift ratio; (c) peak floor total acceleration

sake of completeness, the corresponding 16th (line with cross markers) and 84th (line with square markers) percentiles are also depicted. As can be seen in Figure 2, the two procedures lead to almost identical results. Therefore, on this base, it can be argued that the simplified approach, providing the approximated solutions in Equations (10) and (11), represents a reliable and efficient solution in order to quickly detect the optimal parameters of a TMDI attached to a base-isolation system.

5 | ANALYSIS OF CONTROL PERFORMANCE

On the basis of the results obtained and in order to attest to the effectiveness of the TMDI, the approximate solution is used to design the TMDI in a comparative analysis with other passive control devices. Specifically, the TMDI is compared to the most common devices TMD and TLCD to investigate which of these three devices best performs in terms of base and structural displacement. For the sake of completeness, the comparison is performed through numerical simulations on three different isolated structures to take into account a wide range of structural types. These three structures are characterized by a different number of floors and different stiffness properties and they are denoted as

"flexible five-story base-isolated structure," "stiff 5-story base-isolated structure," and "20-story base-isolated structure," respectively. Specifically, the first case study (i.e., flexible five-story base-isolated structure[23]) concerns with the benchmark structure analyzed in Section 4. The second structure is another five-story isolated building, with a higher stiffness compared to the first one as shown in Adam et al,[32] whereas the third structure refers to a 20-story base-isolated studied in Yang et al.[3] For the passive control devices, the mass ratio is supposed to be the same for all the considered systems (i.e., 5%), and their optimal design parameters have been determined through the same kind optimization procedure considering $G_0 = 0.002$.

In particular, the TMDI and TMD parameters have been determined considering Equations (10) and (11) and assuming $\beta = 0.3$ for the TMDI and the setting $\beta = 0$ for the TMD case. Note that, because Equations (10) and (11) depend only on the mass ratio and the inertance ratio of the considered device, the optimal parameters of TMDI and TMD are the same for all the three structures analyzed in the following. Specifically, the TMDI parameters are $\nu_{d,opt} = 0.781$ and $\zeta_{d,opt} = 0.264$, and the TMD parameters are $\nu_{opt} = 0.940$ and $\zeta_{opt} = 0.109$. As far as the TLCD is concerned, the optimal design parameters are derived as described in other studies[27,28] considering a TLCD with a length ratio $\alpha = 0.8$. Note that, according to previous works,[27,28] the optimal values of the TLCD depend on ζ_b and ω_b, hence, they are different for the three considered structures. In particular, for the flexible five-story base-isolated structure, the tuning ratio is $\nu_{opt} = 0.893$ and the head loss coefficient is $\xi_{opt} = 6.342$, whereas for the stiff five-story base-isolated structure $\nu_{opt} = 0.944$ and $\xi_{opt} = 4.670$ and for the 20-story base-isolated structure $\nu_{opt} = 0.952$ and $\xi_{opt} = 4.802$.

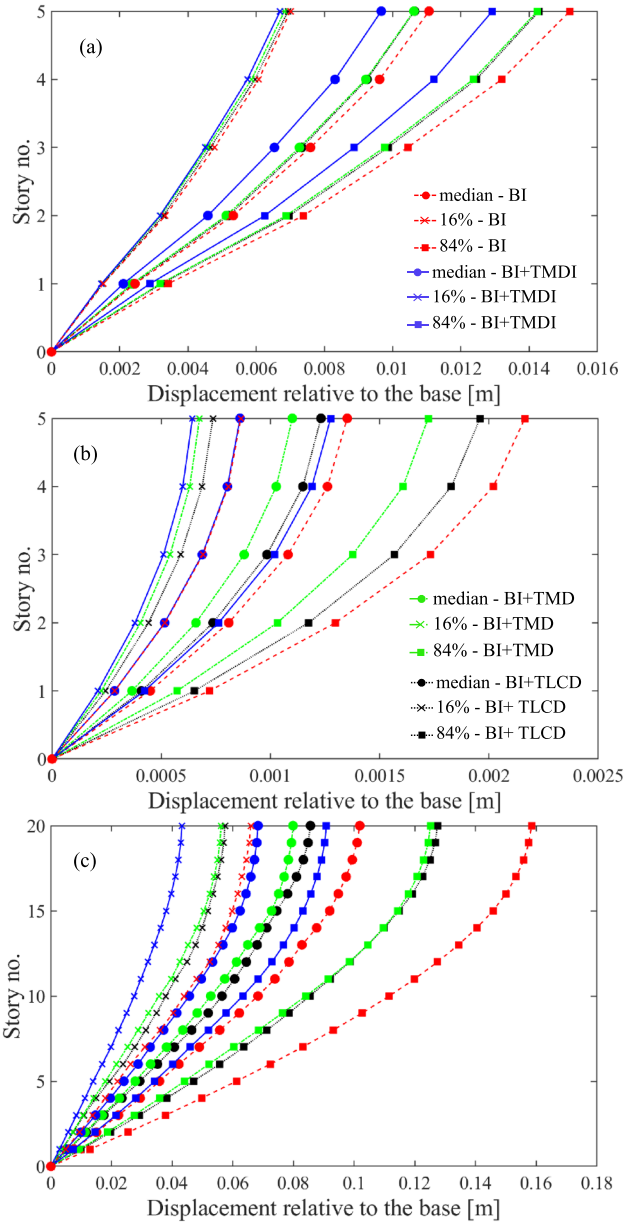

FIGURE 3 Response profiles in terms of peak floor displacement relative to the base for hybrid controlled structure with TLCD (black dotted line), with TMD (green dash-dotted line), with TMDI (blue solid line) and base-isolated structure (red dashed line) subjected to the 44 FEMA P-695-FF records: circles—median; crosses—16th percentile; squares—84th percentiles; (a) flexible five-story base-isolated structure; (b) Stiff five-story base-isolated structure; (c) 20-story base-isolated structure

In this context, Figures 3–5 show the profiles (median, 16th and 84th percentiles) of the peak response quantities of the three types of base-isolated structures without devices (red dashed line), with TLCD (black dotted line), TMD (green dash-dotted line), and TMDI (blue solid line). Specifically, Figures 3–5a refer to the case study of the flexible five-story base-isolated structure, Figures 3–5b to the stiff five-story base-isolated structure, whereas Figures 3–5c to the 20-story base-isolated structure. As it can be seen in Figures 3–5a, the optimized TMDI device in combination with the base-isolation subsystem is able to effectively reduce the relative displacement demand (see Figure 3a) and total accelerations (Figure 5a) of the base-isolated system (red dashed line), and it outperforms the other devices in reducing the structural displacement and acceleration demand. In particular, the median of the peak displacement and acceleration of the fifth floor is reduced by the 13% and 7%, respectively, when the base-isolated structure is endowed with a TMDI compared to the simple base-isolated one. It is also worth stressing that, because the interstory drift ratio decreases when the TMDI is connected to the base-isolation subsystem (see Figure 4a), this reduction is not achieved at its expense, as may be the case when generally providing supplemental damping to the base-isolation subsystem.[33]

In an analogous way, as depicted in Figures 3–5b,c, similar conclusions are suggested from the analysis performed for the two additional isolated structures. As it can be seen, the figures show the higher control performances of the isolated system equipped with the TMDI in reducing the structural responses of the simple base-isolated structure

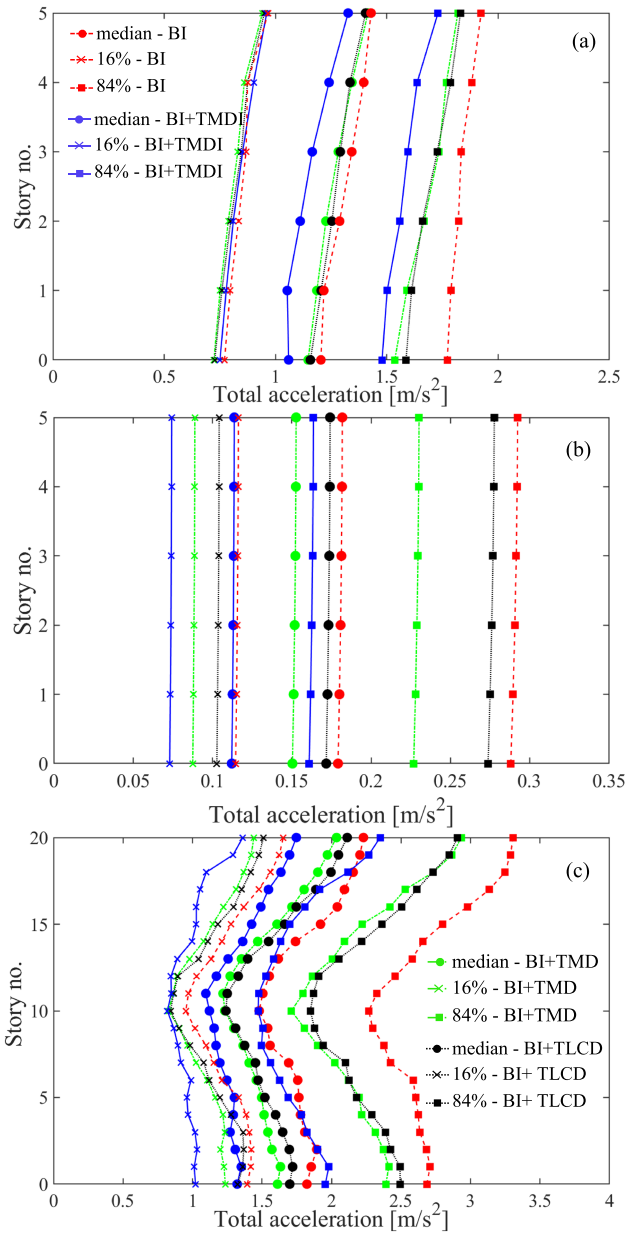

FIGURE 5 Response profiles in terms of peak floor total acceleration for hybrid controlled structure with TLCD (black dotted line), with TMD (green dash-dotted line), with TMDI (blue solid line) and base-isolated structure (red dashed line) subjected to the 44 FEMA P-695-FF records: circles—median; crosses—16th percentile; squares—84th percentiles; (a) Flexible five-story base-isolated structure; (b) Stiff five-story base-isolated structure; (c) 20-story base-isolated structure

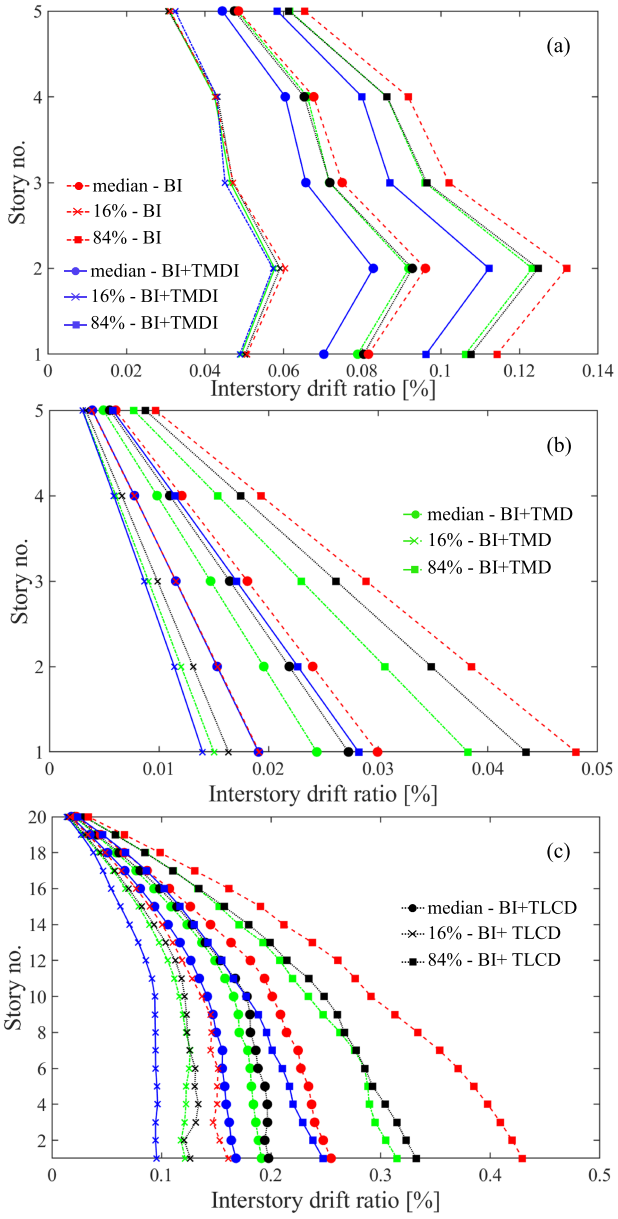

FIGURE 4 Response profiles in terms of peak floor displacement interstory drift ratio for hybrid controlled structure with TLCD (black dotted line), with TMD (green dash-dotted line), with TMDI (blue solid line) and base-isolated structure (red dashed line) subjected to the 44 FEMA P-695-FF records: circles—median; crosses—16th percentile; squares—84th percentiles; (a) Flexible five-story base-isolated structure; (b) Stiff five-story base-isolated structure; (c) 20-story base-isolated structure

compared to the other devices. Specifically, the stiff five-story isolated equipped with a TMDI achieves a reduction of the 19% in terms of median of the peak displacement of the last floor building compared to the base-isolated system, whereas the reduction for the 20-story base-isolated is 33%.

6 | THE EFFECT OF THE DAMPING OF THE BASE-ISOLATION SYSTEM

It is widely known that, although high levels of damping in base-isolation systems contribute to a reduction of base displacement, detrimental effects may arise in the superstructure's response, because interstory drifts and floor accelerations may be increased due to the participation of higher mode responses.[33] To this end, in this section, the effect of increasing the damping ratio of the base-isolation system on the control performance of passive control devices is investigated. In the framework of systems that can be approximated reasonably well by first mode responses and by a rigid structure model, linear isolation systems with moderate isolator damping (<20%) are examined. Specifically, laminated rubber bearings can be modeled as linear systems usually have ζ_b values in the range between 5% (low-damped isolators) and 15% (high-damped isolators). Clearly, at higher values of ζ_b, the governing equations of motion should take into account the nonlinearities that generally characterize heavy-damped isolators. Note that, in this section, the 20-story base-isolated structure previously analyzed and described in Yang et al[3] is considered. A numerical analysis is

carried out on the hybrid controlled 20-story base-isolated structure, considering several cases with higher values of damping up to 15%. The results are reported in terms of interstory drift (Figure 6) and total acceleration (Figure 7). Similar results, not reported for the sake of brevity, have been obtained for the base displacement relative to the base and to the ground. Figures 6 and 7a depict the response profiles of the 20-story base-isolated structure for $\zeta_b = 5\%$. In this case, the reduction by adding the control devices is still significant. Response profiles are also shown for $\zeta_b = 10\%$ in Figures 6 and 7b and for $\zeta_b = 15\%$ in Figures 6 and 7c. The results indicate that with increasing damping ζ_b, the TMDI (blue solid line) becomes less effective. In particular, the interstory drift is almost unaffected by the addition of the device to the base-isolated structure when ζ_b equals 15% (Figure 6c). Similar results are obtained for the TMD (green dash-dotted line) and TLCD (black dotted line). Note that for $\zeta_b = 10\%$ and $\zeta_b = 15\%$, the TMDI is not able to achieve a reduction in terms of total accelerations even compared to the other devices (Figure 7b,c). Hence, on the basis of these outcomes, it can be concluded that equipping isolated systems with a TMDI may be more appropriate for base-isolated structures characterized by values of damping in the base-isolation subsystem lower than 10%.

However, it is worth stressing that combining low-damping conventional isolators (i.e., with $\zeta_b = 5\%$) with the TMDI may be a proper alternative to high-damping base-isolation systems because it leads to better seismic performances. In particular, maximum values (mean from the 44 FEMA P-695-FF records) of the displacement of the base-isolation subsystem, interstory drifts, and the variance of the base displacement are listed in Table 2 for the simple

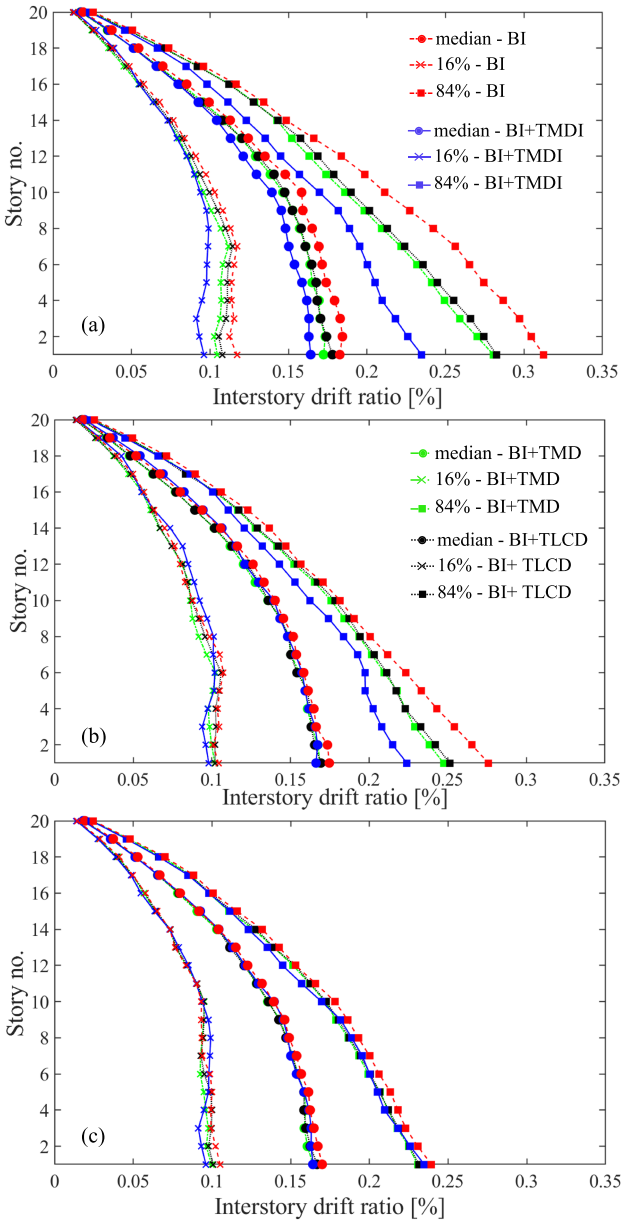

FIGURE 6 Response profiles in terms of peak floor interstory drift ratio for the hybrid controlled 20-story base-isolated structure with TLCD (black dotted line), with TMD (green dash-dotted line), with TMDI (blue solid line) and base-isolated structure (red dashed line) subjected to the 44 FEMA P-695-FF records: circles—median; crosses—16th percentile; squares—84th percentiles; (a) $\zeta_b = 5\%$; (b) $\zeta_b = 10\%$; (c) $\zeta_b = 15\%$

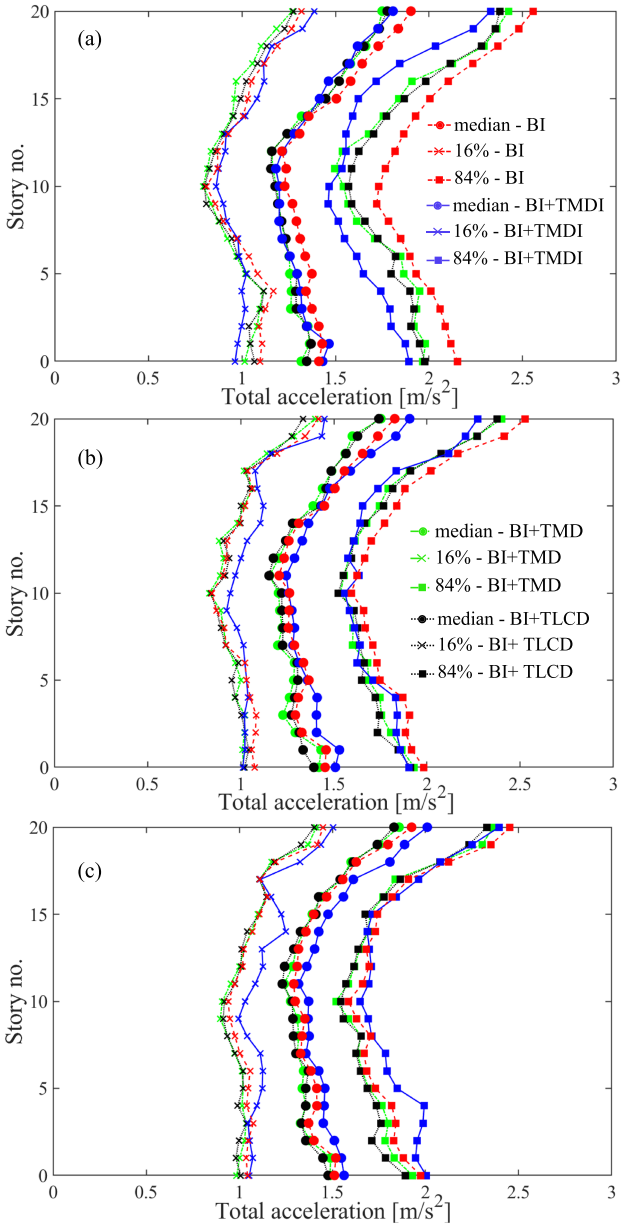

FIGURE 7 Response profiles in terms of peak floor total acceleration for the hybrid controlled 20-story base-isolated structure with TLCD (black dotted line), with TMD (green dash-dotted line), with TMDI (blue solid line) and base-isolated structure (red dashed line) subjected to the 44 FEMA P-695-FF records: circles—median; crosses—16th percentile; squares—84th percentiles; (a) $\zeta_b = 5\%$; (b) $\zeta_b = 10\%$; (c) $\zeta_b = 15\%$

TABLE 2 Maximum values (mean from the 44 FEMA P-695-FF records) of the displacement of the base-isolation subsystem, interstory drift and base displacement variance for two control systems: 20-story base-isolated structure and 20-story base-isolated structure coupled with TMDI

Control system	Max base displacement x_b (m)	Max interstory drift Δ_x (m)	Base displacement variance $\sigma^2_{X_b}$ (m^2)
20-Story base-isolated structure ($\zeta_b = 5\%$)	1.19×10^{-1}	5.47×10^{-4}	6.42×10^{-4}
in conjunction with the TMDI			
20-Story base-isolated structure ($\zeta_b = 15\%$)	1.26×10^{-1}	5.72×10^{-4}	8.07×10^{-4}
without TMDI			

20-story base-isolated structure (without TMDI) with high damping properties ($\zeta_b = 15\%$) and for the same structure with ($\zeta_b = 5\%$) in conjunction with the TMDI. From Table 2, it can be seen that a greater reduction of the base displacement demand, both in terms of maximum value of base displacement and base displacement variance, can be achieved by the isolated system, endowed with low-damping isolators and equipped with the TMDI, rather than the

base-isolated system with high damping properties. Moreover, this reduction is not obtained at the expense of the maximum value of the last interstory drift.

Furthermore, a root mean square (RMS) analysis, carried out to increase the damping ratio of the base-isolated system of the 20-story base-isolated structure subjected to the set of the 44 ground motions,[31] confirms the results previously obtained. Figure 8 represents the median of the RMS base displacement responses (Figure 8a), roof displacement responses (Figure 8b), interstory drifts (Figure 8c), and accelerations (Figure 8d) against the damping coefficient of isolators ζ_b in the range from 0.28% to 15%. When the isolator damping $\zeta_b = 0.28\%$, the TMDI (blue solid line) leads to a reduction of the RMS in terms of base displacement of the 77%, followed by the TMD (green dash-dotted line) with the 60% and by the TLCD (black line) with the 49% (Figure 8a). All the RMSs responses gradually decrease as the base-isolation subsystem damping increases. Thus, the reduction of the structural response provided by the system equipped with the passive control devices may not so significant, especially for values at ζ_b greater than 10%. However, the TMDI (blue solid line), unlike the other devices, shows an approximately constant behavior in reducing the responses in terms of RMSs of the isolated structure (red dashed line), which are almost unaffected by the increase of damping.

Finally, to further show the reliability of these results, a frequency analysis is also performed, in which the damping ratio ζ_b of the 20-story base-isolated structure is increased from the original value (0.28%) to 15%. The structure has been considered subjected to each record from the 44 FEMA P-695-FF ground motions. The average of the frequency response functions (FRFs) of the base displacement responses of the system equipped with the TMDI, the TMD and the TLCD, respectively, is depicted along with that of the simple isolated system for $\zeta_b = 10\%$ and $\zeta_b = 15\%$ in Figure 9a,b, respectively. In general, all the control devices, as shown in Figure 9, are able to reduce the peak of the FRF of the simple base-isolated structure (red dashed line). In Figure 9a, the peak of base displacement FRF of the system equipped with the TMDI (blue solid line), plotted for $\zeta_b = 10\%$, is reduced by almost 60%, compared to the simple base-isolated system (red dashed line). In particular, the FRF of both base displacement of the system equipped with the TMDI (blue

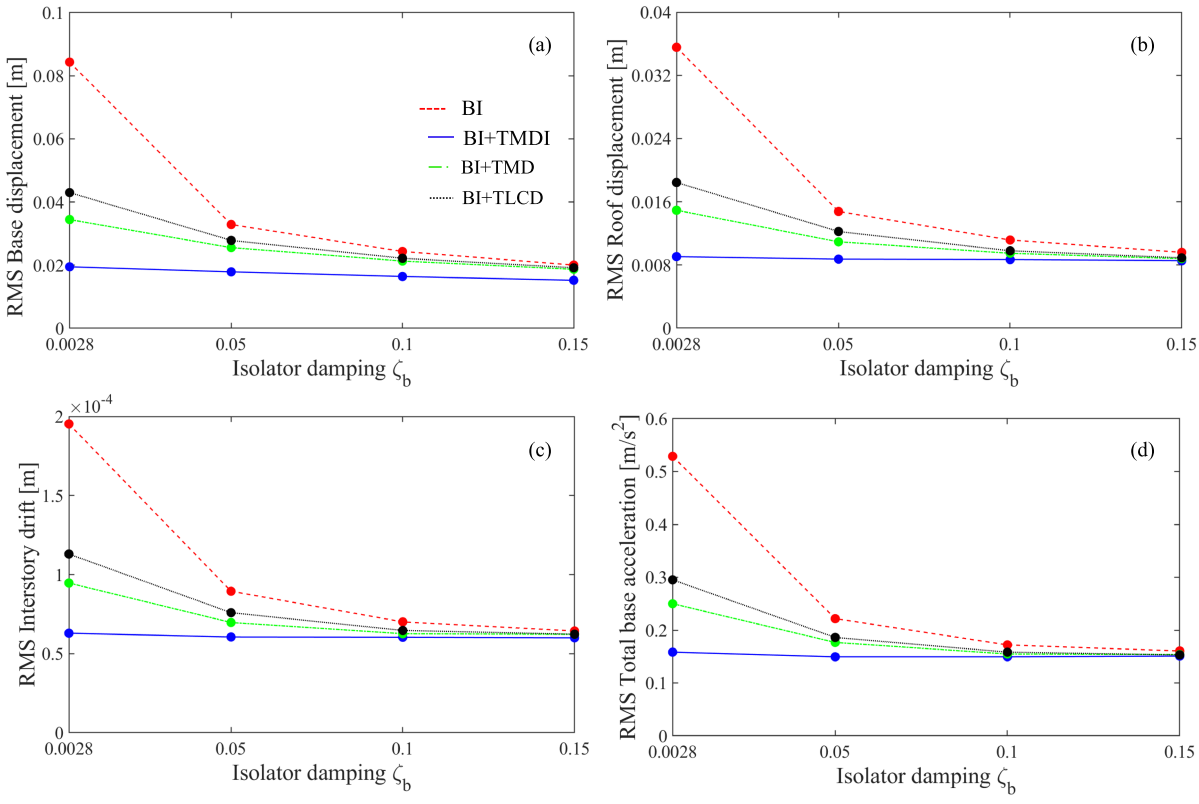

FIGURE 8 Root mean square analysis for the hybrid controlled 20-story base-isolated structure with TLCD (black dotted line), with TMD (green dash-dotted line), with TMDI (blue solid line) and base-isolated structure (red dashed line) subjected to the 44 FEMA P-695-FF records: circles—median; crosses—16th percentile; squares—84th percentiles; (a) base displacement; (b) roof displacement relative to the base; (c) interstory drift; (d) total base acceleration

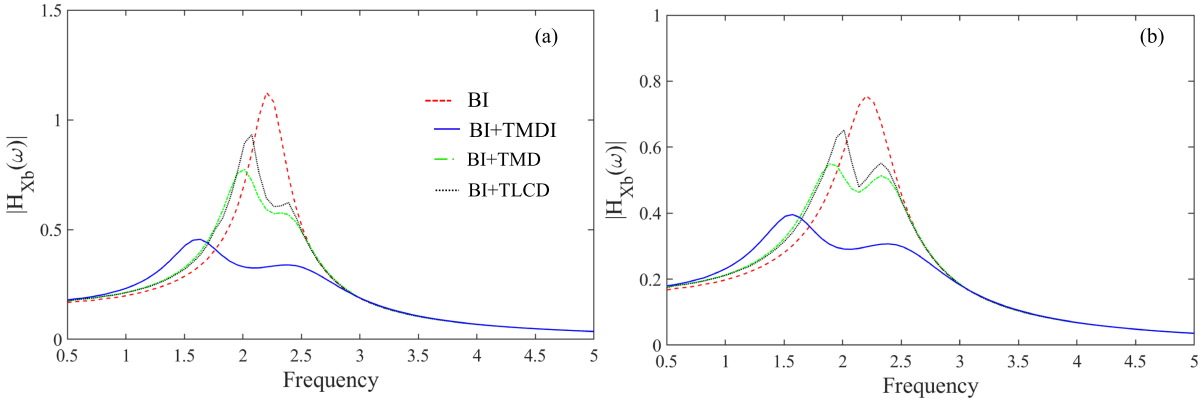

FIGURE 9 Frequency response function in terms of base displacement for the hybrid controlled 20-story base-isolated structure with TLCD (black dotted line), with TMD (green dash-dotted line), with TMDI (blue solid line) and base-isolated structure (red dashed line) subjected to the 44 FEMA P-695-FF records; (a) for $\zeta_b = 10\%$; (b) for $\zeta_b = 15\%$

solid line) is the lowest among the FRFs of the system combined with the other examined devices such as the TMD (green dash-dotted line) and the TLCD (black dotted line). However, as shown in Figure 9b with increasing damping, for the case $\zeta_b = 15\%$, the ability of the passive control devices to suppress the FRF peak of the structural response at the first mode is slightly reduced. Therefore, the TMDI can be considered as an efficient means to improve the dynamic performance of base-isolation systems, especially for low-damped isolated structures (say with a damping coefficient of the base-isolation subsystem $\zeta_b < 10\%$).

7 | CONCLUSIONS

In this paper, the control performance of TMDI attached to base-isolated systems has been thoroughly analyzed. Specifically, a recently proposed simple optimization procedure for quickly finding the optimal TMDI parameters, based on the minimization the base-isolation subsystem displacement variance under Gaussian white noise assumption as base excitation, has been assessed by comparing its results with the outcomes of a more accurate but much more time-consuming optimization technique. In fact, although the simplified procedure proposes simple closed-form formulae based on a straightforward approach, the second one requires a more complex numerical minimization procedure.

The data reveal that both procedures lead to almost identical results, thus showing the reliability and efficiency of the proposed approximate closed-form procedure, despite being based on some assumptions. Further, an analysis has been carried out to verify the reliability of the approximate closed-form optimization procedure for different types of structures. Specifically, three TMDI controlled base-isolated structures, characterized by different stiffness properties and height, have been analyzed subjected to a collection of 44 ground motions with different features. Furthermore, the case of the TMDI with the base-isolation was also compared with other hybrid control strategies such as the base-isolated system in combination with the traditional TMD and the TLCD. Structural responses in the form of displacements, accelerations, and interstory drift demonstrate the effectiveness achieved by the TMDI over the TMD and the TLCD in improving the seismic performance of the base-isolation.

Numerical simulations, carried out to study the effect of increased damping of the base-isolation subsystem to take into account the case of high-damped base-isolated structures, indicate that the TMDI is particularly efficient in controlling the structural quantities (displacements, accelerations, and interstory drift) of isolated structures when low damping isolators are employed. Therefore, the use of a TMDI coupled with low damped isolated structures is proposed as an appealing alternative to high damped isolated structures since the TMDI shows a greater reduction of base displacements while maintaining the small interstory drifts typical of isolated structures.

From a practical point of view, no "grounded" inerter has been installed in civil structures yet, whereas cases with the traditional TMD coupled with base isolation systems already exist.[34,35] Moreover, as far as the practical realization of the inerter is concerned, the current trend of literature suggests the use of ball screw inerters to avoid detrimental features such as backlash effects.[36-38]

ACKNOWLEDGEMENTS

A. Di Matteo, C. Masnata, and A. Pirrotta gratefully acknowledge the support received from the Italian Ministry of University and Research, through the PRIN 2017 funding scheme (project 2017J4EAYB 002 - Multiscale Innovative Materials and Structures "MIMS"). A. Di Matteo gratefully acknowledge the financial support of the project PON R&I 2014-2020-AIM (Attraction and International Mobility), project AIM1845825-1.

ORCID

Christoph Adam https://orcid.org/0000-0001-9408-6439

REFERENCES

1. Naeim F, Kelly JM. *Design of Seismic Isolated Structures: From Theory to Practice*. New York: John Wiley & Sons; 1999.
2. Kelly JM. Base isolation: linear theory and design. *Earthq Spectra*. 1990;6(2):223-244.
3. Yang JN, Danielians A, Liu SC. Aseismic hybrid control systems for building structures. *J Eng Mech*. 1991;117(4):836-853.
4. Palazzo B, Petti L. Seismic response control in base-isolated systems using tuned mass dampers. In: Proceedings of the first world conference on structural control; 1994; Los Angeles, CA.
5. Tsai H-C. The effect of tuned-mass dampers on the seismic response of base-isolated structures. *Int J Solids Struct*. 1995;32(8):1195-1210.
6. Xiang P, Nishitani A. Optimum design for more effective tuned mass damper system and its application to base-isolated buildings. *Struct Control Health Monit*. 2014;21(1):98-114.
7. Melkumyan MG. New concept of a dynamic damper to restrict the displacements of seismically isolated buildings. In: Proc. international conference on advances in materials science and engineering; Seoul, Korea; 2012:1-5.
8. Petti L, Giannattasio G, Iuliis MD, Palazzo B. Small scale experimental testing to verify the effectiveness of the base isolation and tuned mass dampers combined control strategy. *Smart Struct Syst*. 2010;6:57-72.
9. Kareem A. Modelling of base-isolated buildings with passive dampers under winds. *J Wind Eng Indust Aerodyn*. 1997;72:323-333.
10. Taniguchi T, Kiureghian AD, Melkumyan M. Effect of tuned mass damper on displacement demand of base-isolated structures. *Eng Struct*. 2008;30(12):3478-3488.
11. Love JS, Tait MJ, Toopchi-Nezhad H. A hybrid structural control system using a tuned liquid damper to reduce the wind induced motion of a base isolated structure. *Eng Struct*. 2011;33(3):738-746.
12. Di Matteo A, Furtmüller T, Adam C, Pirrotta A. Optimal design of tuned liquid column dampers for seismic response control of base-isolated structures. *Acta Mech*. 2018;229(2):437-454.
13. Hochrainer MJ. Tuned liquid column damper for structural control. *Acta Mech*. 2005;175(1):57-76.
14. Di Matteo A, Lo Iacono F, Navarra G, Pirrotta A. Innovative modeling of tuned liquid column damper controlled structures. *Smart Struct Syst*. 2016;18:117-138.
15. Di Matteo A, Lo Iacono F, Navarra G, Pirrotta A. Experimental validation of a direct pre-design formula for TLCD. *Eng Struct*. 2014;75:528-538.
16. Furtmüller T, Di Matteo A, Adam C, Pirrotta A. Base-isolated structure equipped with tuned liquid column damper: an experimental study. *Mech Syst Signal Process*. 2019;116:816-831.
17. Smith MC. Synthesis of mechanical networks: The inerter. *IEEE Trans Autom Control*. 2002;47(10):1648-1662.
18. Papageorgiou C, Houghton NE, Smith MC. Experimental testing and analysis of inerter devices. *J Dyn Syst Measurement Control*. 2008;131(1):11001.
19. Li C, Liang M, Wang Y, Dong Y. Vibration suppression using two-terminal flywheel. Part I: Modeling and characterization. *J Vibr Control*. 2012;18(8):1096-1105.
20. Domenico DD, Deastra P, Ricciardi G, Sims ND, Wagg DJ. Novel fluid inerter based tuned mass dampers for optimised structural control of base-isolated buildings. *J Franklin Institute*. 2019;356(14):7626-7649.
21. Saitoh M. On the performance of gyro-mass devices for displacement mitigation in base isolation systems. *Struct Control Health Monit*. 2012;19(2):246-259.
22. Hashimoto T, Fujita K, Tsuji M, Takewaki I. Innovative base-isolated building with large mass-ratio TMD at basement for greater earthquake resilience. *Future Cities Environ*. 2015;1(1):9.
23. De Domenico D, Ricciardi G. An enhanced base isolation system equipped with optimal tuned mass damper inerter (TMDI). *Earthq Eng Struct Dyn*. 2018;47(5):1169-1192.
24. Marian L, Giaralis A. Optimal design of a novel tuned mass-damper–inerter (TMDI) passive vibration control configuration for stochastically support-excited structural systems. *Probabilistic Eng Mech*. 2014;38:156-164.
25. Angelis MD, Giaralis A, Petrini F, Pietrosanti D. Optimal tuning and assessment of inertial dampers with grounded inerter for vibration control of seismically excited base-isolated systems. *Eng Struct*. 2019;196:109250.
26. Di Matteo A, Masnata C, Pirrotta A. Simplified analytical solution for the optimal design of tuned mass damper inerter for base isolated structures. *Mech Syst Signal Process*. 2019;134:106337.
27. Di Matteo A, Lo Iacono F, Navarra G, Pirrotta A. Optimal tuning of tuned liquid column damper systems in random vibration by means of an approximate formulation. *Meccanica*. 2015;50(3):795-808.
28. Di Matteo A, Lo Iacono F, Navarra G, Pirrotta A. Direct evaluation of the equivalent linear damping for TLCD systems in random vibration for pre-design purposes. *Int J Non-Linear Mech*. 2014;63:19-30.

29. Roberts JB, Spanos PD. *Random vibration and statistical linearization*. Mineola: Dover Publications; 2003.
30. Perez RE, Behdinan K. Particle swarm approach for structural design optimization. *Comput Struct*. 2007;85(19):1579-1588.
31. FEMA P-695. Quantification of building seismic performance factors technical representative Federal Emergency Agency. Washington, DC; 2009.
32. Adam C, Di Matteo A, Furtmüller T, Pirrotta A. Earthquake excited base-isolated structures protected by tuned liquid column dampers: design approach and experimental verification. *Procedia Eng*. 2017;199:1574-1579.
33. Kelly JM. The role of damping in seismic isolation. *Earthq Eng Struct Dyn*. 1999;28(1):3-20.
34. tech. rep.
35. Melkumyan MG. Concepts of dampers for earthquake protection of existing buildings and for displacements restraints in seismically isolated buildings. In: 1st Pan-American Congress on Computational Mechanics; Seoul, Korea; 2015:1-12.
36. Madhamshetty KMJM. Low-rate characterization of a mechanical inerter. *Machines*. 2018;6:32.
37. Sun HWXPJWW. Exact h2 optimal solutions to inerter-based isolation systems for building structures. *Struct Control Health Monit*. 2019;26:e2357.
38. Qian FSHTWZL. Optimal tuned inerter dampers for performance enhancement of vibration isolation. *Eng Struct*. 2019;198:1-14.

How to cite this article: Masnata C, Di Matteo A, Adam C, Pirrotta A. Assessment of the tuned mass damper inerter for seismic response control of base-isolated structures. *Struct Control Health Monit*. 2021;28:e2665. https://doi.org/10.1002/stc.2665

APPENDIX A: SIGMA POINTS GENERATION SCHEMES

In this appendix, the displacement transfer functions of the system Equation (2) are presented. In this respect, applying the Fourier transform of system Equation (2) results in

$$\begin{aligned} X_b(\omega)\left[-\omega^2(1+\mu_d+\beta)+2i\omega\zeta_b\omega_b+\omega_b^2\right]-\omega^2(1+\mu_d)X_d(\omega)-\omega^2\frac{1}{M_{tot}}\mathbf{r}^T\mathbf{M}\mathbf{X}(\omega)&=-(1+\mu_d)\ddot{X}_g(\omega),\\ -\omega^2X_b(\omega)+X_d(\omega)\left[-\omega^2+2i\omega\zeta_d\omega_d+\omega_d^2\right]&=-\frac{\mu_d}{\mu_d+\beta}\ddot{X}_g(\omega),\\ -\omega^2\mathbf{M}\mathbf{r}X_b(\omega)+\left[-\omega^2\mathbf{M}+i\omega\mathbf{C}+\mathbf{K}\right]\mathbf{X}(\omega)&=-\mathbf{M}\mathbf{r}\ddot{X}_g(\omega). \end{aligned} \tag{A1}$$

Therefore, the base-isolation displacement transfer function $H_{X_b}(\omega)$ of the system equipped with TMDI can be written as

$$H_{X_b}(\omega)=\frac{X_b(\omega)}{\ddot{X}_g(\omega)}=\frac{(1+\mu_d)+\frac{^{\omega}\mu_d}{c(\omega)}+\omega^2\frac{1}{M_{tot}}\mathbf{r}^T\mathbf{M}\mathbf{a}(\omega)\mathbf{M}\mathbf{r}}{-b(\omega)+\frac{\omega^4(\mu_d+\beta)}{c(\omega)}+\omega^4\frac{1}{M_{tot}}\mathbf{r}^T\mathbf{M}\mathbf{a}(\omega)\mathbf{M}\mathbf{r}}, \tag{A2}$$

whereas the main structure displacement transfer function $H_{\mathbf{X}}(\omega)$ and TMDI displacement transfer function $H_{X_d}(\omega)$, respectively, are

$$H_{\mathbf{X}}(\omega)=\frac{\mathbf{X}(\omega)}{\ddot{X}_g(\omega)}=\mathbf{a}(\omega)\left[-\mathbf{M}\mathbf{r}+\omega^2\mathbf{M}\mathbf{r}H_{X_b}(\omega)\right],\ H_{X_d}(\omega)=\frac{1}{c(\omega)}\left[-\frac{\mu_d}{\mu_d+\beta}+\omega^2H_{X_b}(\omega)\right], \tag{A3}$$

$$\mathbf{a}(\omega)=\left[-\omega^2\mathbf{M}+i\omega\mathbf{C}+\mathbf{K}\right]^{-1},\ b(\omega)=-\omega^2(1+\mu_d+\beta)+i\omega2\zeta_b\omega_b+\omega_b^2,\ c(\omega)=-\omega^2+2i\omega\zeta_d\omega_d+{\omega_d}^2. \tag{A4}$$

It is recalled that by setting β to zero, the correspondent equations of the base-isolated system coupled with the traditional TMD are derived.